

A quantitative method for measuring nanocomposite dispersion

H.S. Khare, D.L. Burris*

Department of Mechanical Engineering, University of Delaware, Newark, DE 19716, USA

ARTICLE INFO

Article history:

Received 6 December 2009

Accepted 23 December 2009

Available online 4 January 2010

Keywords:

Nanocomposite

Dispersion

Reinforcement

ABSTRACT

The materials science community has identified nanoparticle dispersion as a primary challenge area for the advancement of polymer nanocomposites technology. Although nanoparticle dispersion can significantly impact important engineering properties, it is not itself a quantifiable property; qualitative TEM image assessments remain as the 'gold standard' for dispersion characterization. While numerous quantitative dispersion analyses have been proposed, they have often proven cumbersome, system specific and unreflective of the proposed benefits of nanoparticle reinforcement. No single quantitative method has been adopted by the community to date and inferences about processing and dispersion effects generally require subjective analysis. This paper presents a quantitative dispersion characterization method which 1) makes use of standard TEM dispersion images; 2) directly reflects proposed nanoscale reinforcement mechanisms; 3) outputs a single performance metric. By quantitatively isolating dispersion effects, this technique may help to link disparate studies in the literature while providing defensible quantitative insights into nanoscale reinforcement mechanisms.

© 2009 Elsevier Ltd. All rights reserved.

1. Introduction

Fiber and fabric composites derive unrivalled strength and stiffness per unit mass from synergies between lightweight polymeric matrices and moderate to high loadings of oriented fillers with exceptional tensile strength and stiffness. Despite the unique performance attributes of these materials, inherent processing challenges limit their usefulness in the consumer marketplace where mass production is a primary functional requirement. These materials are not strongly sensitive to filler size, yet there is evidence that even trace additions of nanoscale fillers can significantly improve the properties of a polymer matrix. There are substantial scientific and practical interests in these nanomaterials for their potential to transfer into the bulk of everyday products [1].

The successful transfer of nanocomposite technology requires the development of a more fundamental understanding of the reinforcement mechanisms. Nanostructured materials are difficult to characterize and many aspects of these systems are unclear at present. Prior works have attributed nanofiller reinforcement of polymers to numerous mechanical factors including filler debonding, crack pinning, thin layer yielding and interfacial load transfer [2–7]. For example, Fiedler et al. [8] noted that micro-reinforcement mechanisms, including crack deflection and filler–polymer debonding, stem directly from reduced filler size and

improved dispersions with reduced agglomerations. Other investigators have found evidence that the interface between filler and matrix can have long-range impacts on nearby polymer chains; this region is known by several names including interphase, interfacial zone and interfacial region [3,4,9]. Overwhelmingly, the research suggests that filler size, loading and distribution dictate the amount of affected polymer [10–12], while the surface structure and chemistry of the particles dictate the intensity of interaction at the particle/polymer interface [13,14].

Intuition suggests that reinforcement increases as the filler loading increases. Numerous investigators have demonstrated improved properties with increased loadings [5,11,15–21]. Often, however, these benefits are limited to loadings below an optimum whereby additional loadings are detrimental. Qualitatively, the optimums coincide with the emergence of significant agglomeration of the nanoparticles; there have been no systematic investigations of this effect due primarily to the absence of a robust and quantitative dispersion characterization tool. The literature clearly demonstrates that optimum performance requires an effective distribution of the nanoparticles within the matrix. However, the same scaling effects that make nanoparticles attractive also compete against effective dispersion. Nanoparticles tend to 'stick' to one another and are difficult to separate or disperse due to high specific surface area and energy. The more they interact with one another, the less they interact with the polymer in need of reinforcement. These nanoparticle agglomerations have little cohesive strength and their presence is often detrimental to the properties

* Corresponding author. Tel.: +1 302 831 2006.

E-mail address: dlburris@udel.edu (D.L. Burris).

being targeted for improvement [19]. Increased loadings of **effectively** dispersed particles increase the interaction volume and contribute to additional reinforcement. Review articles of the field have consistently cited nanoparticle dispersion as a major challenge area for the advancement of polymer nanocomposite technology [11,12,22,23].

Despite the broadly recognized importance of nanoparticle dispersion, the characterization of dispersion remains largely qualitative and based on subjective interpretations of standard transmission electron microscopy (TEM) images. Myriad quantitative methods have been proposed [24–37], but none have been widely implemented due to deficiencies in generality and simplicity.

Jordan et al. [14] and Burriss et al. [38] assembled general trends from the literature, but noted inconsistencies and even contradictory trends in the published literature. The development of a simple and broadly applicable dispersion quantification technique will clarify such occurrences while promoting a more fundamental understanding of polymer nanocomposite materials and reinforcement mechanisms. By quantitatively measuring dispersion, systematic studies of processing, loading, particle size, agglomeration and interfacial interaction effects become possible. This paper describes the development of a quantitative dispersion characterization tool that, 1) utilizes the state of the art TEM images that presently pervade the literature, 2) appropriately reflects hypothesized reinforcement mechanisms and 3) has a single, physically intuitive output metric. It is anticipated that this technique will help to isolate processing and dispersion effects from interfacial effects, link disparate studies in the literature and provide general insights into nanoscale reinforcement mechanisms.

2. Experimental

2.1. Background: the uniform distribution as a dispersion characterize tool

The uniform distribution is often used to characterize the optimal dispersion. In this model, each filler particle is equidistant from its four nearest neighbors as shown in Fig. 1a. This dispersion minimizes the size of the unreinforced polymer domains and effectively compartmentalizes damage; presumably, inferior properties of the polymer matrix have motivated reinforcement. A number of investigators have found direct or indirect evidence

that the particle/polymer interface can have a ‘long-range’ impact on the local polymer chains [39–44]. The volume of reinforced or affected polymer is optimized if these regions do not overlap. As illustrated in Fig. 1b, even slight clustering results in a significant increase in the size of the unreinforced domains and a significant reduction in the affected polymer volume.

There is little question that a uniform dispersion provides efficient reinforcement. The benefits of the uniform dispersion are so intuitive that justification rarely accompanies assertions that uniform is optimal. Many of the quantitative dispersion characterization methods involve measures of the average deviation from uniformity which may be defined in a number of ways [26,29–31]. However, simple comparisons against a uniform distribution provide little insight into nanoscale reinforcement phenomena. Such methods have two important flaws for the purposes of understanding polymer nanocomposite behavior. First, the use of nanoparticle reinforcement is fundamentally motivated by size-scaling arguments, yet a ‘uniform distribution’, per se, is length-scale independent. Further, the ‘uniform distribution’ is independent of any measure of the density or sparsity of dispersion. Such a tool would therefore favor the use of microparticles over nanoparticles due to their relative ease of dispersion. Filler size and loading are fundamentally related to the properties of the nanocomposite and must be addressed if the method is to be useful in a broad sense.

Loading and scaling effects are illustrated in Fig. 2. All four dispersions are perfectly uniform, but intuitively, one might expect different properties due to differences in the reinforcement states. The dispersion in Fig. 2a has the largest domains of unreinforced polymer. Increasing loading by 4× in Fig. 2b reduces the unreinforced domain length by 65% and the unreinforced domain volume by 96%. Conversely, if loading is held constant, a 50% reduction in filler size has the same effect. Reducing particle size is theoretically the most efficient means for polymer reinforcement. If particle size is reduced by an order of magnitude (e.g. 1 μm particles replaced by 100 nm particles), the average volume of the unreinforced polymer domains is reduced by three orders of magnitude. This critical effect is completely neglected by typical dispersion metrics.

2.2. Inter-particle distance as a dispersion characterization tool

The distance between particles reflects the size of unreinforced polymer and provides a scale-dependent measure of the dispersion

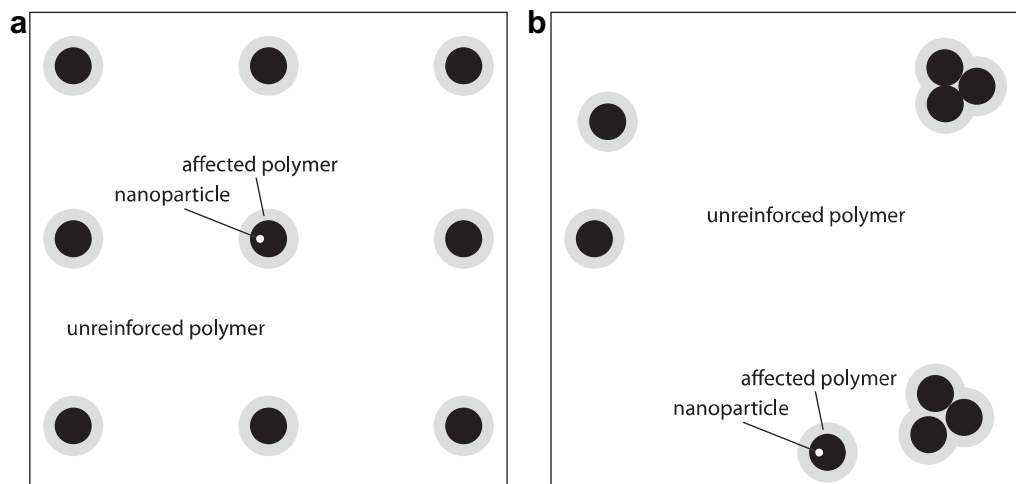


Fig. 1. Illustrations of two possible dispersion states for nanoparticles within a polymer matrix: a) a uniform dispersion, b) a more realistic dispersion with two small clusters of particles. Deviations from uniformity reduce the volume of the reinforced polymer and increase the size of the unreinforced polymer domains.

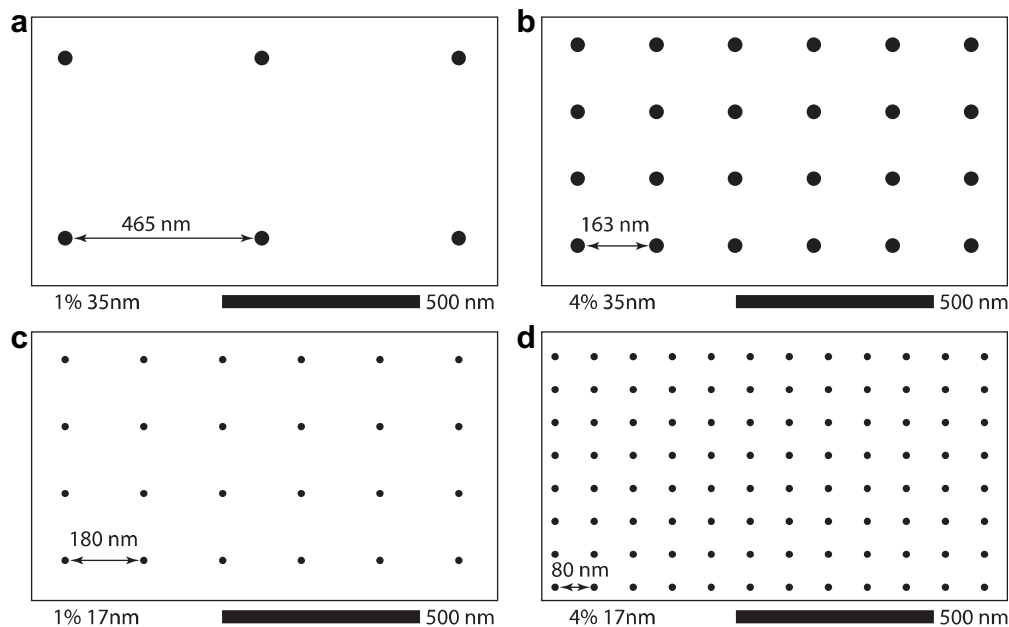


Fig. 2. Four uniform dispersions illustrating the effects of filler size and loading: a) the particles in the top row are twice the diameter of those on the bottom; the loading in the left column is constant at 1% while the loading on the right is constant at 4%. Under constant dispersion and loading conditions, reductions in filler diameter also reduce the size of the unreinforced polymer domains. Multiplying loading by 4× has the same effect as dividing size by 2×.

state. Basu et al., Xie et al. and Hamming et al. [24,45,46] use the mean inter-particle distance (average distance between every possible combination of particles) to serve as a measure of exfoliation. This method is sensitive to the number of particles, but is rather insensitive to dispersion quality. This is illustrated by the hypothetical dispersions in Fig. 3; although the dispersion on the right is significantly more agglomerated, this technique would yield similar values for the inter-particle distance; the smaller inter-particle distances within one agglomerate negate the larger

distances between agglomerates. The inter-particle distance, in this case, reflects the number of particles rather than the distribution of particles.

Luo and Koo [29–31] developed an interesting technique that addresses the inherent challenges of complex particle fields. They suggest characterizing the size of the unreinforced domains of polymers rather than the distribution of particles. This method identifies the unreinforced polymer as the weak link and therefore provides a more direct measure of the important physical factors

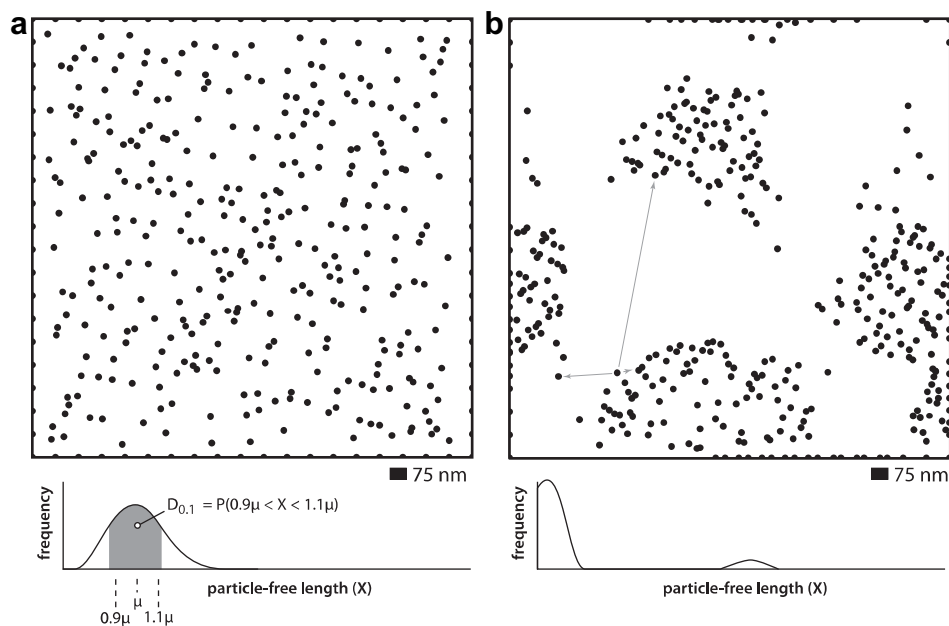


Fig. 3. Illustrations of two hypothetical dispersions with the same particles: a) a non-agglomerated dispersion; b) an agglomerated dispersion. The mean inter-particle distance from Basu and Xie [24,45] is similar for a) and b) despite obvious and important qualitative differences in the dispersion states. Approximate histograms using the method from Luo and Koo [29–31] are provided below the dispersions. Both methods note the importance of the particle-free space; the method from Basu and Xie [24,45] is insensitive to dispersion quality and agglomerations while the method from Luo and Koo is scale independent.

like filler dispersion, loading and size. First, the size of each particle-free domain is measured to generate a histogram of domain sizes. A normal or lognormal distribution is then fit to the data. The performance metric, $D_{0,1}$, is the integral from 0.9μ to 1.1μ of the fitted distribution, where μ is the mean inter-particle distance. This method is similar to the aforementioned uniformity measures and essentially measures deviation from average behavior to indicate dispersion quality; similarly, this method is scale and particle-density independent and cannot, therefore, account for potential nanoscale reinforcement mechanisms.

3. Results

3.1. Method: free-space length, L_f

At the most fundamental level, nanoscale reinforcement originates at the interface of the particle and polymer [9,13,19]. These nanoscopic interactions are only useful if they compound to produce macroscopically significant modifications to engineering properties. The distribution, or dispersion, of the particles dictates the degree to which the nanoscale interactions impact macroscale properties. The important characteristics of the dispersion depend on the distribution (in a dimensionless sense), particle size and particle loading, but to date, no single technique has quantitatively accounted for all three. The goal in this paper is to interpret dispersion and facilitate quantitative studies of particle processing, size, loading and interfacial reinforcement.

The largest characteristic domains of unreinforced polymer constitute the weak link of the nanocomposite; these unreinforced regions are expected to behave as the neat polymer and will thus limit the macroscale performance [47]. The most direct performance metric is the characteristic size of the unreinforced polymer domains, which is referred to here as the free-space length, L_f . As dispersion becomes more uniform for constant filler loading and size, L_f is reduced. As particle size is reduced for a given distribution and loading, L_f is reduced. As loading is increased for a given particle size and distribution, L_f is reduced. This parameter directly measures the effects of variables that are empirically known to impact the macroscopic mechanical properties.

The suggested method for obtaining L_f begins with a representative TEM image of the nanocomposite of interest (Fig. 4). This initial step is ubiquitous to other qualitative and quantitative methods in the literature. This image is subsequently converted to a black and white bitmap where black distinguishes the filler from the matrix (in white). Visual inspection of Fig. 4 reveals one large agglomeration, many smaller clusters, individual particles and significant variability in the inter-particle free-space. These imperfections are typical and illustrate the complexities of nanoparticle dispersions. Visual inspection suggests a characteristic free-space length on the order of 500 nm.

Reconsider the random particle field of Fig. 3a. For a random distribution of events (particles in this case), the Poisson distribution describes the probability of an event occurring over some random observation interval. It is described mathematically by the probability density function,

$$f(k, \lambda) = \frac{e^{-\lambda} \lambda^k}{k!} \quad (1)$$

where f is the probability, k is the actual number of occurrences and λ is the expected number of occurrences. The free-space length is defined here as the length of the largest observation area for which the most probable number of intersecting particles is zero. The Poisson distribution can be directly applied to determine the free-space; the mode of the Poisson distribution approaches zero as λ approaches one. In this case, 30 nm particles are dispersed at 6% loading over the $4 \times 10^6 \text{ nm}^2$ field of view which yields a particle sparsity of $11,700 \text{ nm}^2/\text{particle}$. Thus, $\lambda = 1$ when the observation area is $11,700 \text{ nm}^2$, or when the observation length is $L_f = 108 \text{ nm}$.

While the Poisson distribution is a convenient analytical means for computing L_f , it is of little use in practice where truly random dispersions are rare. As a result, computational means are often necessary. There are several ways to define a robust computational measurement of the free-space length from black and white bitmaps; Luo and Koo [29–31] determined the free-space size histogram as an intermediate step to obtaining $D_{0,1}$. The largest mode is clearly related to the characteristic inter-particle free-space. The free-space length is defined here as the width of the largest randomly placed square for which the most probable number of

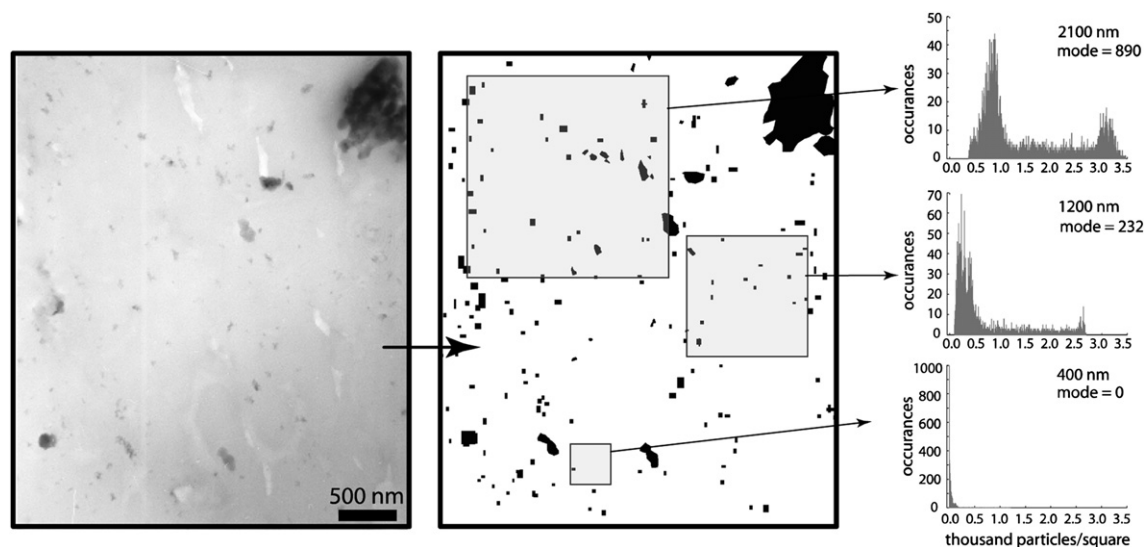


Fig. 4. Illustration of the technique used to calculate the free-space length. Statistically significant numbers of squares of length, L , are placed randomly across the image in order to obtain a histogram of particle frequency per $L \times L$ square. The free-space length is the largest square size for which the most probable number of intersecting particles in a randomly placed square is zero (TEM image from Burriss et al. [48]).

intersecting particles is zero; this is equivalent to the use of the Poisson distribution for random systems. We have written a simple MATLAB™ code to perform this computation; the code can be found with a detailed explanation at the following web page: <http://research.me.udel.edu/~dlburriss/software/dispersion.html>. Initially, a square of length, L , is randomly placed on the image. The number of intersecting particles is counted and stored. This procedure is repeated a statistically significant number of times (10,000 in the case of Fig. 4) and the particle occurrence histogram is used to compute the mode (most probable number of intersecting particles) for the characteristic square length, L . The code iterates on square size to find the largest square for which the most probable number of intersecting particles in a randomly placed square is zero. It is important to note that the method is valid for any distribution of particles.

The method is illustrated in Fig. 4. For a length of 2100 nm, the most probable number of particles per square is 890; any number larger than zero indicates that the square is larger than the characteristic length of the particle-free domains. The most probable number of particles for a 1200 nm square is 232. The most probable number of particles for the 400 nm square is zero; the free-space length can be no less than 400 nm. Any smaller square size will also yield a mode at zero. For ten repeat measurements, the method converges on $L_f = 540 \text{ nm} \pm 21 \text{ nm}$.

The results of this analysis can be compared to those of the Poisson distribution as a measure of the dispersion efficiency. The

particles in this study have an average diameter of 40 nm. Five percent of the field of the $1.4 \times 10^7 \text{ nm}^2$ field of view contains particles. The number of expected occurrences is one for an area of $32,000 \text{ nm}^2$. Thus, the free-space length of a truly random distribution of the same particles would be 178 nm. The difference between the Poisson analysis and the actual computation is due to the inevitable clustering and agglomerations that occurs in practice. A comparison between L_f and the limiting value from the Poisson distribution gives a more traditional measure of the dispersion quality without regard to filler size or loading.

3.2. Trends with controlled dispersions

The uniform dispersion is unrealistic but useful for descriptive purposes due to its simplicity and prevalence in the literature. The dispersion in Fig. 5a is a uniform dispersion of 30 nm particles at 6% loading. The field of view is $2 \mu\text{m}$ and the particle center-to-center distance is 105 nm. The distance between particle edges is 75 nm. The statistical simulation method yields a free-space length of 73 nm. Even though larger squares will fit between particles, the probability is below the minimum threshold needed to produce a zero mode. As the box size is reduced, it becomes more likely that randomly placed boxes will fit interstitially. The free-space length is clearly and fundamentally linked to the characteristic size of the unreinforced polymer domains; values of L_f for uniform dispersions can be measured by inspection to a very good approximation.

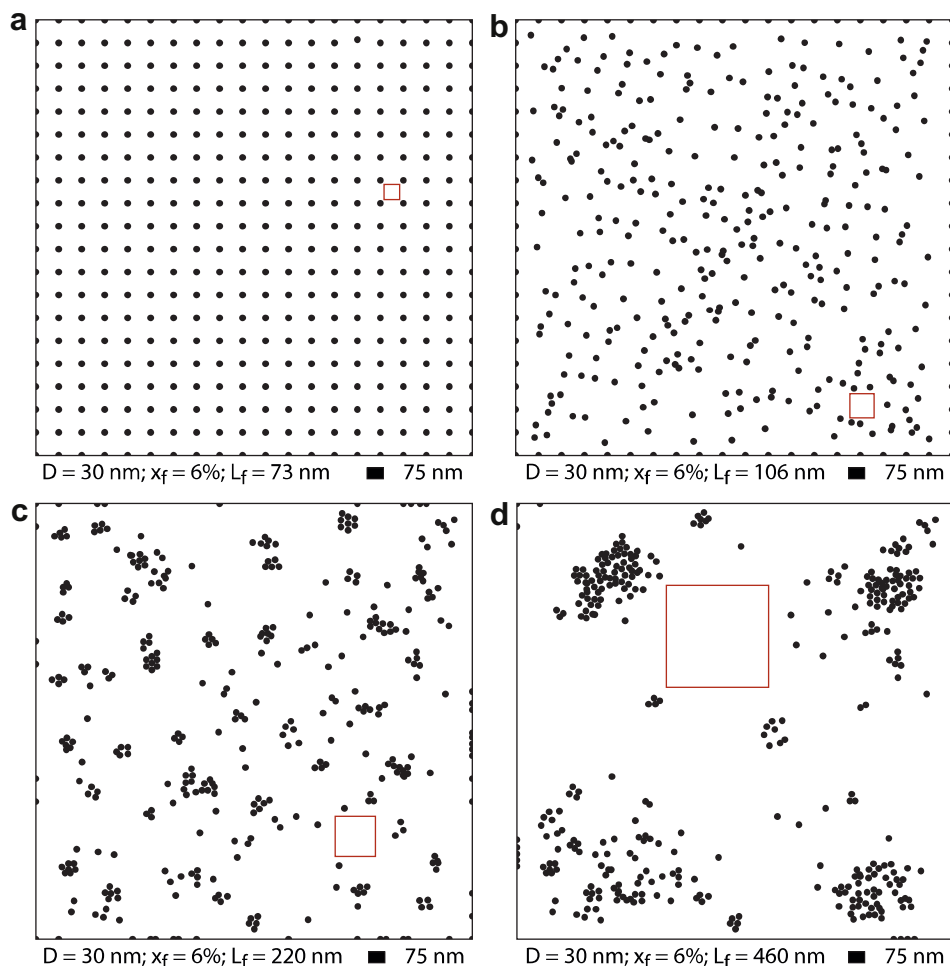


Fig. 5. Varying dispersions of 30 nm particles at 6% loading a) uniform dispersion – $L_f = 73 \text{ nm}$; b) random dispersion – $L_f = 106 \text{ nm}$; c) clustered dispersion – $L_f = 220 \text{ nm}$; d) agglomerated dispersion – $L_f = 460 \text{ nm}$. Open squares have a length equal to the free-space length which increases as the dispersion worsens.

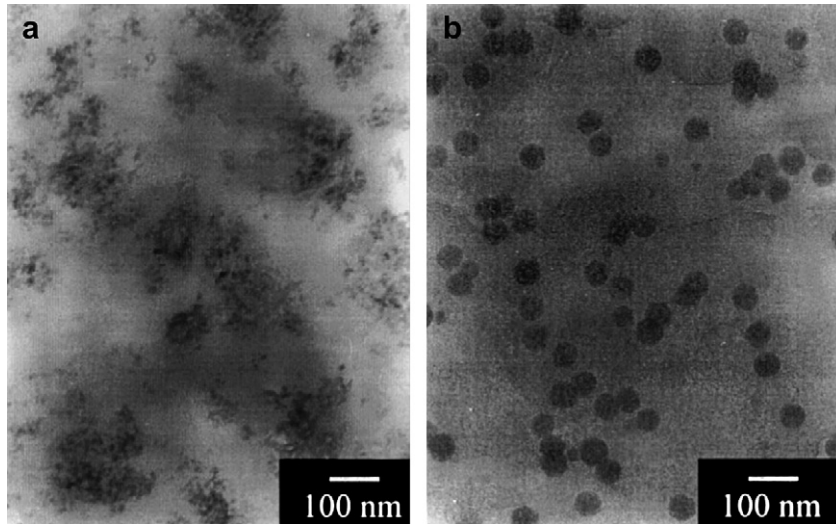


Fig. 6. TEM images of silica/PAG nanocomposites with (a) 17 nm silica particles (b) 50 nm silica particles; with a filler loading of 5% in each case [4].

As shown in Fig. 2, reduced particle size or increased particle loading reduces the free-space length. The controlled dispersions of Fig. 5 illustrate the effect of dispersion on free-space length. Randomizing the uniform particle field in Fig. 5a increases the free-space length from 73 nm to 106 nm; the Poisson distribution yields $L_f = 108$ nm. In practice, it is exceptionally difficult to achieve random dispersions of nanoparticles due to low mass, high surface energy and an increasingly strong driving force toward clustering and agglomeration with reduced filler diameter. Nanoparticles are frequently found to cluster or agglomerate without assistance from surfactants which generally impact the interface between polymer and filler. The small clustering in Fig. 5c increases the free-space length to 220 nm and agglomeration in Fig. 5d increases the free-space length to 460 nm. This trend clearly illustrates the benefits of

the uniform dispersion and the detrimental impact of nanoparticle agglomeration. Particle size, loading and dispersion are coupled and difficult to isolate without quantitative dispersion characterization tools.

4. Discussion

4.1. Agglomeration effects and trends with varied loadings

The success of a dispersion characterization tool can be measured by its ability to explain trends from prior works, forecast improvements or detriments and offer insights into design directions for optimum performance. The present method is unique in that it reflects idealized trends in nanofillers dispersion, size and

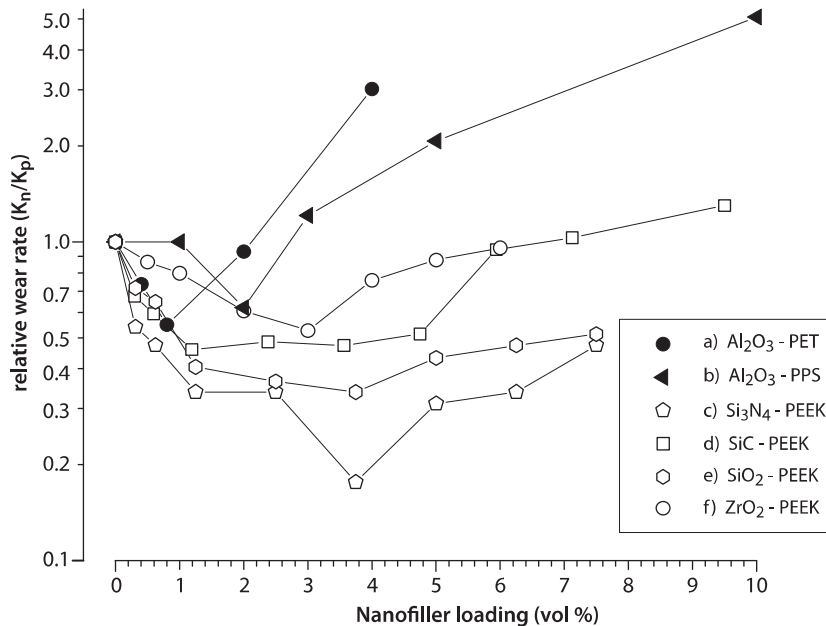


Fig. 7. Relative wear-rate plotted versus nanofillers loading for solid lubricant nanocomposites in the literature: a) Al₂O₃/PET nanocomposite Bhimaraj et al. [49]; b) Al₂O₃/PPS nanocomposite Schwartz and Bahadur [50]; c) Si₃N₄/PEEK nanocomposite Wang et al. [51,54]; d) SiC/PEEK nanocomposite Wang et al. [52]; e) SiO₂/PEEK nanocomposite Wang et al. [53]; f) ZrO₂/PEEK nanocomposite Wang et al. [51,54]. In every case, there is a trend of decreased wear rate with increased filler loading until a critical loading where further additions are detrimental.

loading; as dispersion state is improved, nanoparticle size reduced or loading increased, the free-space length is reduced. A contradiction arises with the emergence of agglomerations. It is unclear at what point the detrimental effects of agglomerations begin to outweigh the benefits of reduced free-space length as particle loading is increased or as particle size is reduced.

Agglomerations are likely responsible for the ubiquitous presence of optimal loadings in the polymer nanocomposites literature; as fillers are added, properties are improved up to the optimum whereby further additions become detrimental. This phenomenon is clearly illustrated by the solid lubricant wear-rate literature. Polymers lack sufficiently low friction and wear, so fillers are required to reinforce the matrix and facilitate the formation of protective transfer films. Reinforcing microfillers abrade these films and the countersurfaces both of which accelerate wear. Nanoparticles are ideal for addressing the unique challenges of solid lubrication.

Relative wear-rates are plotted versus nanofiller loading for solid lubricant nanocomposites from the tribology literature in Fig. 7 [49–54]. The relative wear rate is defined as the ratio of the composite wear rate to the matrix wear rate and provides an indication of reinforcement. Despite wide variations in the materials, synthesis and testing conditions between studies, their results offer similar trends. As small amounts of nanofillers are added to polymer matrices, wear rate is reduced. In every case, there exists an optimal loading.

Wear improvements, optimal loadings and the degree to which wear rate increases above the optimum are system dependent; it is unclear if these important factors are driven by the interactions of filler and matrix, dispersion, synthesis or testing conditions. Wang et al. [51–54] held the dispersion method and matrix material constant for data sets c)–f). Optimal loadings were similar while the improvement in wear rate varied from 2× to 5×. Dispersion analyses were not conducted for these materials. Studies by Bhimaraj

et al. [49] and Schwartz and Bahadur [50] demonstrated optimums at much lower loadings and significantly increased wear above the optimum. In both cases, the authors noted the appearance of nanoparticle agglomerates at loadings above the optimum during SEM observation of the transfer films. It is very possible, if not likely, that wear improvements in these cases were limited by dispersion and an inability to avoid agglomerates when reducing L_f with higher loadings. The relationship between wear rate and dispersion remains unclear to date, although Burris et al. [48] found evidence of reduced wear rate when a low surface energy treatment was used to reduce agglomeration (it should be noted that the treatment effect on dispersion could not be separated from the effect on the interface).

Similar trends are observed in the general polymer nanocomposite literature [5,6,11,15,16,18,19,21]. Chen et al. [55] observed optimums and dispersion states during a study of the tensile and thermal properties of γ -alumina–epoxy nanocomposites. The authors found that 5 phr (parts per hundred resin) filler loading produced the highest modulus, elongation to failure and thermal stability. The authors used TEM observation to study the effect of dispersion; the images from the study are shown in Figs. 8 and 9. It can be seen that L_f is reduced monotonically with increased loading, which contradicts the assertion that the free-space length is the primary dispersion-related factor in determining nanoscale reinforcement. In addition to reduced L_f , however, the authors noted increased aggregation with increased loading and offered an agglomerate-based hypothesis to explain the optimum. Qualitatively, the dispersion of the 9 phr sample appears quite poor, and it is not difficult to imagine that the most favorable failure pathway may transition from the unreinforced matrix at 5 phr to the large and weak agglomerates found at 9 phr.

The following model is consistent with the general trends in the literature: when agglomerations are small relative to the free-space, the unreinforced polymer constitutes the most favorable

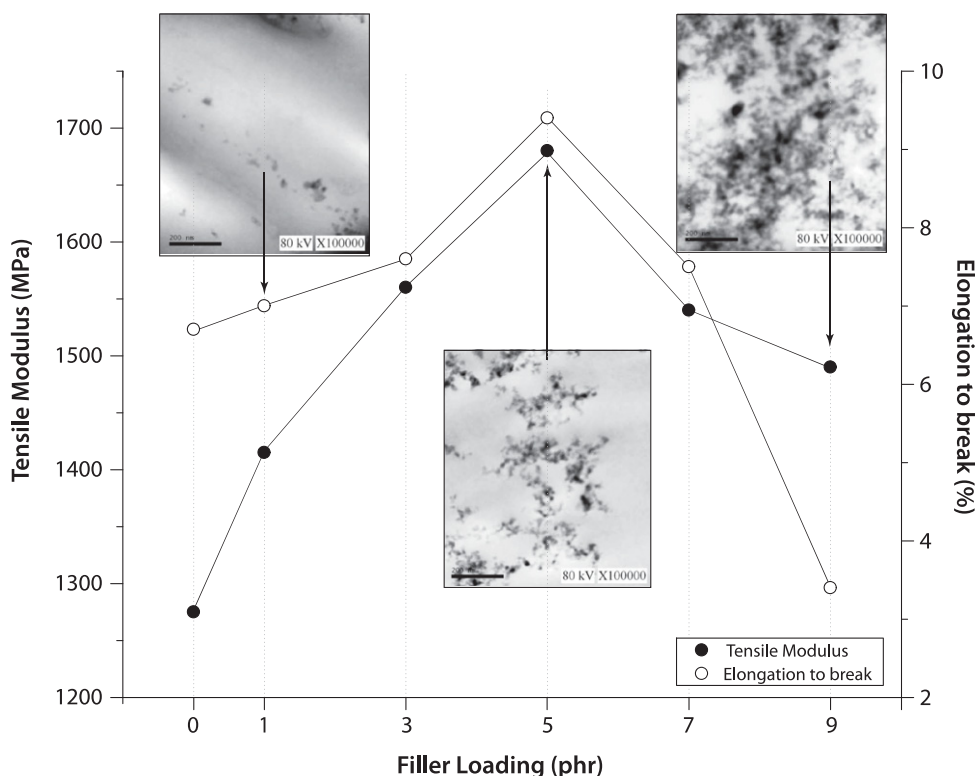


Fig. 8. Tensile modulus, elongation to break and corresponding dispersions for nanocomposites from Chen et al. [55].

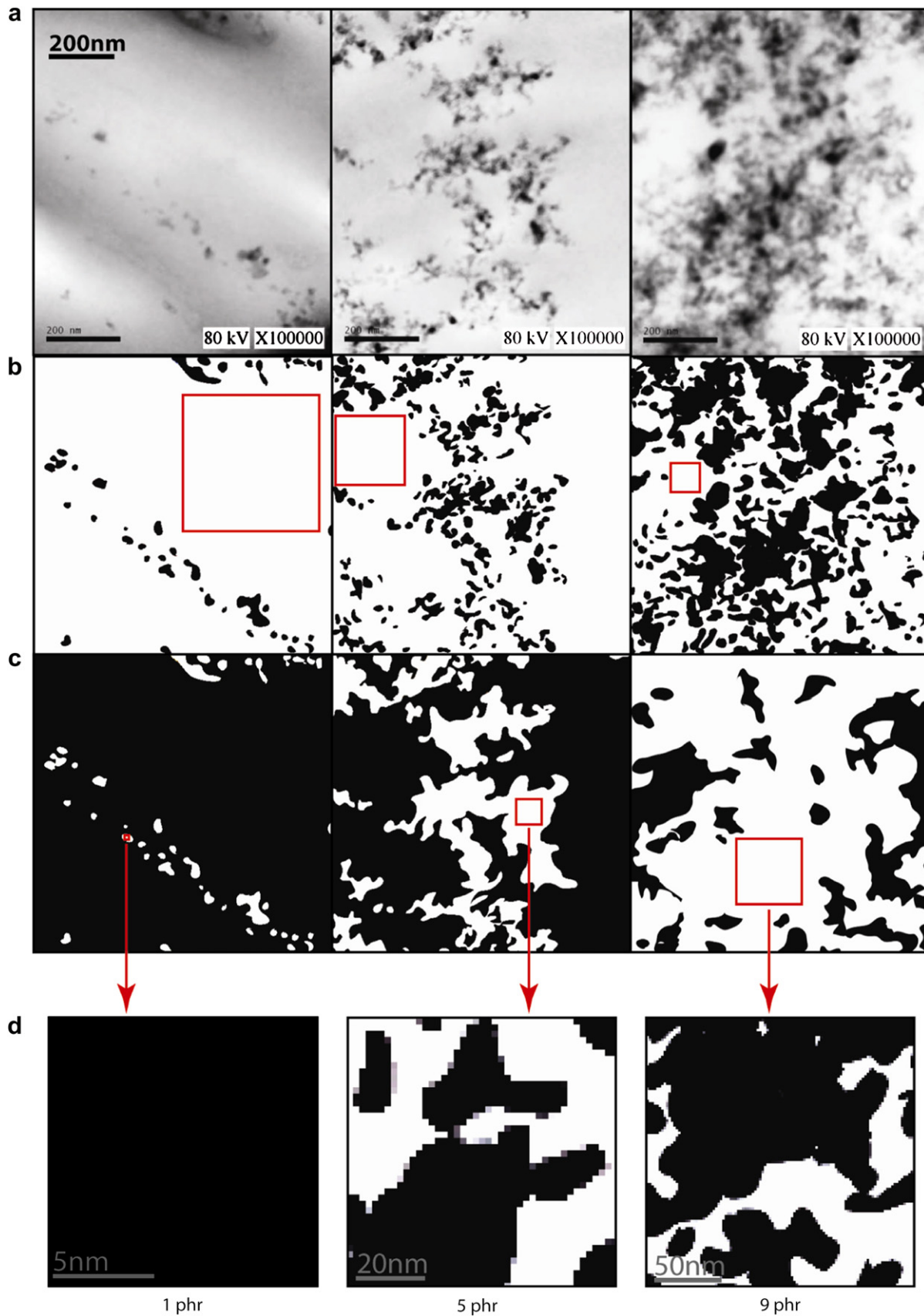


Fig. 9. Three loading-varied dispersions of γ -alumina in epoxy at 1, 5 and 9 phr from Chen et al. [55]. Figures corresponding to each dispersion indicate: (a) the original TEM micrographs; (b) L_f boxes overlaid on converted black/white images. Values of L_f for each are: 415 nm, 211 nm, 89 nm; (c) L_a boxes overlaid on converted black/white images, with values of L_a as 13 nm, 78 nm, 200 nm; (d) Enlarged view of the agglomeration box in (c) for each loading, indicating the area fractions within agglomerations.

failure pathway. In this case, it is the size of this unreinforced region which governs damage compartmentalization and the degree of nanoscale reinforcement over macroscopic length-scales. When agglomerations become large relative to the free-space, they become the most favorable location for failure which results in macroscopically degraded properties. Agglomerations, in effect, modify the effective free-space length. The effective free-space length, L_f^* , is the equivalent free-space length for infinitely small agglomerations and the following form is qualitatively consistent with the observations of the literature. L_f^* is defined as,

$$L_f^* = L_f \left[1 + \left(\frac{1}{a} \frac{L_a}{L_f} \right)^n \right] \quad (2)$$

where L_a is the agglomeration length, a is the critical ratio of agglomeration length to free-space length, and n is a sensitivity exponent. Generally, the modified free-space length is insensitive to agglomeration size as long as the agglomerations are smaller than the free-space length; thus, as one adds filler to reduce free-space at the expense of increased agglomeration size (1–5 ph Chen et al.), performance is expected to improve until these lengths become comparable. In this case, $a = 1$. In other cases, performance may become susceptible to agglomerations more quickly, for example, as the agglomerations approach half the free-space length. In this case, $a = 1/2$.

Agglomerates are only qualitatively defined as ensembles of nanoparticles. To be consistent with the preceding method, an agglomerate is defined here as any continuous region where the characteristic spacing between individual particles is less than the characteristic particle diameter. The treatment for calculating the agglomeration length, L_a , is exactly the same as that used to quantify L_f . First, the image is converted into a black and white bitmap where black now represents unfilled polymer and white represents agglomerates. It is important that the agglomerate (white) contains both matrix and filler over regions where the definition of an agglomerate has been met. The simulation described earlier is then performed to quantify the largest box size for which there is a mode at zero. The conversions and results for dispersions from Chen et al. are shown in Fig. 9.

The nature of the dispersion within agglomerates may prove to have a secondary effect on reinforcement. In this case, one could modify the computed agglomeration length by the area fraction of particles within the agglomerate, as illustrated by Fig. 9d. This

effect will likely prove insignificant with more detailed investigation.

The exponent, n , defines the sensitivity of the effective free-space length to the relative size of the agglomerates and free-space. For $n = 0$, L_f is independent of the agglomeration size as could be the case for a property like bulk modulus. If $n = 1$, $L_f^* = L_f + L_a$. In this case, L_f^* is insensitive to L_a if $L_a < L_f$. However, for a given agglomeration size, this relationship implies that smaller L_f always provides smaller L_f^* . Experience with many engineering properties suggests a penalty for extreme values of L_a/L_f which is likely related to inferior properties of the agglomerates in comparison to the unfilled matrix. For example, a composite with 1 μm agglomerates spaced 5 μm apart ($L_f^* = 6 \mu\text{m}$) might be expected to outperform a composite with 1 μm agglomerates spaced 5 nm apart ($L_f^* = 1.005 \mu\text{m}$). Using $n = 2$ solves the discrepancy; $L_f^* = 5.2 \mu\text{m}$ for the former while $L_f^* = 200 \mu\text{m}$ for the latter. Improving the tuning of this parameter further will require more systematic investigations.

It is evident from Fig. 8 that elongation to break and tensile modulus exhibit different sensitivities to agglomerations and require unique values for n . One could argue that tensile modulus, being derived during elastic deformation, would be expected to be less sensitive to agglomerations than elongation to failure which occurs after gross plastic deformation. The modified free-space length effectively reflects the mechanical properties when $n = 1.5$ for tensile modulus and $n = 2.5$ for elongation to break as shown in Fig. 10. Determining these relationships and values of n more exactly will require more systematic investigation.

A similar design issue arises with attempts to reduce the free-space length with reduced filler size. As stated earlier, particles size reduction is the most efficient means for reducing L_f for a given distribution. Unfortunately, particle size and distribution are coupled, and as particle size is reduced, there is an increased tendency for agglomeration. This issue is exemplified by the work of Reynaud et al. [4] in which two silica particle sizes were dispersed at 5% loading within PA6 using an identical processing method; the TEM dispersion images are shown in Fig. 6. While 50 nm particles were found without significant agglomeration, 17 nm particles dispersed under identical conditions were found to be more agglomerated. Interestingly, trends are similar to those of Chen et al. in that the agglomerated material had a lower elongation to failure but similar modulus. The modified free-space length ($n = 2.5$) is approximately 40% greater and the elongation to failure about 50% lower while modulus and modified free-space length

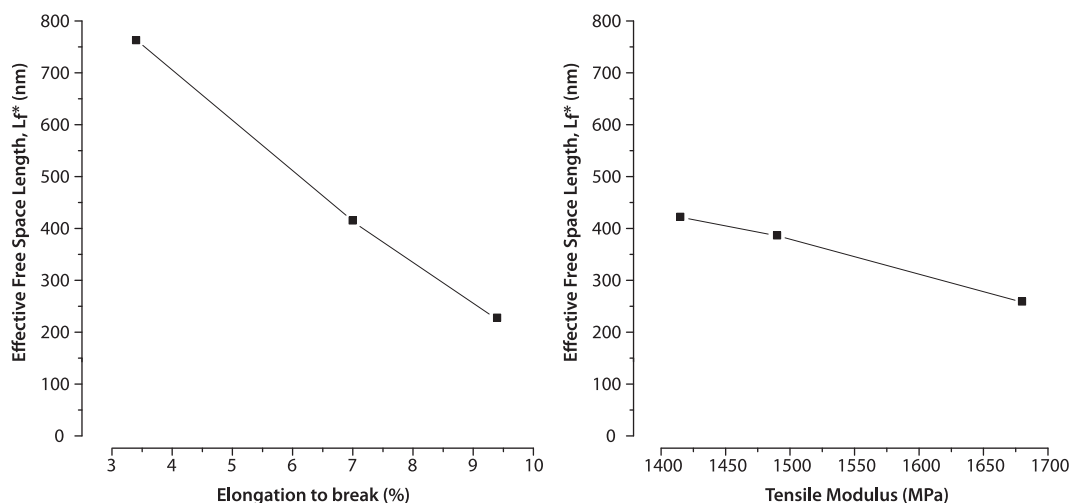


Fig. 10. Variation of effective free space length with elongation to break ($n = 2.5$), and tensile modulus ($n = 1.5$), for the dispersions corresponding to Fig. 9 (see Table 1).

Table 1

Values of tensile modulus, elongation to break, free space and agglomeration lengths for the dispersions of Fig. 9.

Loading (phr)	Tensile modulus (MPa)	Elongation to break (%)	L_f (nm)	L_a (nm)
1	1415	7	415	13
5	1680	9.4	211	78
9	1491	3.4	89	200

($n = 1.5$) remained approximately constant. While smaller particles offer the **potential** for reduced free-space length and improved properties, there is a general competition between reduced free-space length and increased agglomeration.

5. Closing remarks

The materials science community broadly acknowledges the important effects of processing, dispersion and interface effects on the properties of a nanocomposite material. However, the absence of a simple and quantitative dispersion characterization tool has precluded systematic studies of these relationships. To date, the community has lacked insights for material design directions and apparent contradictions in the literature have unclear sources that are likely related to uncharacterized differences in dispersions. Several quantitative dispersion characterization strategies have been proposed, but none have been widely adopted due largely to insensitivities to fundamental characteristics like dispersion state, particle-density and length-scale. They are often developed to respond to a specific system and are of limited value for application to the more general field of literature. The free-space length method presented here is simple, intuitive, quantitative and sensitive to dispersion state, density and length-scale. It utilizes existing TEM image analysis methods and was developed based on broad and well-established trends in the literature. Its output has demonstrated relationships with mechanical properties like elongation to break and tensile modulus. The detrimental effects of agglomerations, which become significant when their characteristic size approaches the free-space length, are effectively accounted for using the modified free-space length. There is strong evidence to suggest that the optimum loadings that are overwhelmingly observed in variable loading studies are due to a competition between reduced free-space length and increased agglomeration with increased loading. It is only through the application of broadly applicable dispersion quantification methods that the effects of processing and dispersion can be systematically probed. The broad applicability of this method will prove useful for studying the effects of processing on dispersion and dispersion on mechanical properties. By understanding and isolating the effects of dispersion, the method may also provide general quantitative insights into nanoscale reinforcement mechanisms which originate at the interface of particle and polymer.

Acknowledgements

This research was carried out with the support of the University of Delaware Research Foundation. We would also like to thank Prof. W.G. Sawyer and Dr. B. Boesl for many helpful discussions regarding the dispersion characterization needs of the nanocomposites field.

References

- [1] Hussain F, Hojjati M, Okamoto M, Gorga RE. *Journal of Composite Materials* 2006;40(17):1511–75.
- [2] Kelly A. *Proceedings of the Royal Society of London. Series A, Mathematical and Physical Sciences* 1970;319(1536):95–116.
- [3] Cotterell B, Chia JYH, Hbaieb K. *Engineering Fracture Mechanics* 2007;74(7):1054–78.
- [4] Reynaud E, Jouen T, Gauthier C, Vigier G, Varlet J. *Polymer* 2001;42(21):8759–68.
- [5] Singh RP, Zhang M, Chan D. *Journal of Materials Science* 2002;37(4):781–8.
- [6] Wichmann MHG, Schulte K, Wagner HD. *Composites Science and Technology* 2008;68(1):329–31.
- [7] Michler GH, Adhikari R, Henning S. *Macromolecular Symposia* 2004;214:47–71.
- [8] Fiedler B, Gojny FH, Wichmann MHG, Nolte MCM, Schulte K. *Composites Science and Technology* 2006;66(16):3115–25.
- [9] Dasari A, Yu ZZ, Mai YW. *Materials Science and Engineering R – Reports* 2009;63(2):31–80.
- [10] Qian D, Dickey EC, Andrews R, Rantell T. *Applied Physics Letters* 2000;76(20):2868–70.
- [11] Thostenson ET, Li CY, Chou TW. *Composites Science and Technology* 2005;65(3–4):491–516.
- [12] Thostenson ET, Ren ZF, Chou TW. *Composites Science and Technology* 2001;61(13):1899–912.
- [13] Gersappe D. *Physical Review Letters* 2002;89(5).
- [14] Jordan J, Jacob KI, Tannenbaum R, Sharaf MA, Jasiuk I. *Materials Science and Engineering A – Structural Materials Properties Microstructure and Processing* 2005;393(1–2):1–11.
- [15] Chang JH, An YU. *Journal of Polymer Science Part B – Polymer Physics* 2002;40(7):670–7.
- [16] Gojny FH, Wichmann MHG, Fiedler B, Schulte K. *Composites Science and Technology* 2005;65(15–16):2300–13.
- [17] He P, Gao Y, Lian J, Wang L, Qian D, Zhao J, et al. *Composites Part A – Applied Science and Manufacturing* 2006;37(9):1270–5.
- [18] Li JX, Silverstein M, Hiltner A, Baer E. *Journal of Applied Polymer Science* 1994;52(2):255–67.
- [19] Rong MZ, Zhang MQ, Zheng YX, Zeng HM, Walter R, Friedrich K. *Polymer* 2001;42(1):167–83.
- [20] Sumita M, Shizuma T, Miyasaka K, Ishikawa K. *Journal of Macromolecular Science – Physics* 1983;B22(4):601–18.
- [21] Wang Y, Huang JS. *Journal of Applied Polymer Science* 1996;60(11):1779–91.
- [22] Gacitua WE, Ballerini AA, Zhang J. *Maderas: Ciencia y tecnología* 2005;7(3):159–78.
- [23] Njuguna J, Pielichowski K. *Advanced Engineering Materials* 2004;6(4):193–203.
- [24] Basu SK, Tewari A, Fasulo PD, Rodgers WR. *Applied Physics Letters* 2007;91(5).
- [25] Fagan JA, Landi BJ, Mandelbaum I, Simpson JR, Bajpai V, Bauer BJ, et al. *Journal of Physical Chemistry B* 2006;110(47):23801–5.
- [26] Kashiwagi T, Fagan J, Douglas JF, Yamamoto K, Heckert AN, Leigh SD, et al. *Polymer* 2007;48(16):4855–66.
- [27] Li ZF, Luo GH, Zhou WP, Wei F, Xiang R, Liu YP. *Nanotechnology* 2006;17(15):3692–8.
- [28] Lillehei PT, Kim JW, Gibbons LJ, Park C. *Nanotechnology* 2009;20(32).
- [29] Luo ZP, Koo JH. *Journal of Microscopy – Oxford* 2007;225(2):118–25.
- [30] Luo ZP, Koo JH. *Polymer* 2008;49(7):1841–52.
- [31] Luo ZP, Koo JH. *Materials Letters* 2008;62(20):3493–6.
- [32] Navarchian AH, Majdzadeh-Ardakani K. *Journal of Applied Polymer Science* 2009;114(1):531–42.
- [33] Pegel S, Potschke P, Villmow T, Stoyan D, Heinrich G. *Polymer* 2009;50(9):2123–32.
- [34] Tscheschel A, Lacayo J, Stoyan D. *Journal of Microscopy – Oxford* 2005;217:75–82.
- [35] Vermogen A, Masenelli-Varlot K, Seguela R, Duchet-Rumeau J, Boucard S, Prele P. *Macromolecules* 2005;38(23):9661–9.
- [36] Wu D, Gao D, Mayo SC, Gotama J, Way C. *Composites Science and Technology* 2008;68(1):178–85.
- [37] Zhou YX, Jeelani MI, Jeelani S. *Materials Science and Engineering A – Structural Materials Properties Microstructure and Processing* 2009;506(1–2):39–44.
- [38] Burriss DL, Boesl B, Bourne GR, Sawyer WG. *Macromolecular Materials and Engineering* 2007;292(4):387–402.
- [39] Papakonstantopoulos GJ, Doxastakis M, Nealey PF, Barrat JL, de Pablo JJ. *Physical Review E* 2007;75(3).
- [40] Sternstein S, Ramorino G, Jiang B, Zhu A. *Rubber Chemistry and Technology* 2005;78(2):258–70.
- [41] Zhu A, Sternstein S. *Composites Science and Technology* 2003;63(8):1113–26.
- [42] Herve E, Zaoui A. *International Journal of Engineering Science* 1993;31(1):1–10.
- [43] Ash B, Schadler L, Siegel R. *Materials Letters* 2002;55(1–2):83–7.
- [44] Eitan A, Fisher F, Andrews R, Brinson L, Schadler L. *Composites Science and Technology* 2006;66(9):1162–73.
- [45] Xie S, Harkin-Jones E, Shen Y, Hornsby P, McAfee M, McNally T, et al. *Materials Letters*;64(2):185–8.
- [46] Hamming LM, Qiao R, Messersmith PB, Brinson LC. *Composites Science and Technology* 2009;69(11–12):1880–6.
- [47] Bahadur S, Gong D. *Wear* 1992;158(1–2):41–59.

- [48] Burris DL, Zhao S, Duncan R, Lowitz J, Perry SS, Schadler LS. A route to wear resistant PTFE via trace loadings of functionalized nanofillers. 2009;267: 653–60.
- [49] Bhimaraj P, Burris DL, Action J, Sawyer WG, Toney CG, Siegel RW, et al. Wear 2005;258(9):1437–43.
- [50] Schwartz C, Bahadur S. Wear 2000;237(2):261–73.
- [51] Wang Q, Xu J, Shen W, Liu W. Wear 1996;196(1–2):82–6.
- [52] Wang Q, Xue Q, Liu W, Chen J. Wear 2000;243(1–2):140–6.
- [53] Wang O, Xue Q, Shen W. Tribology International 1997;30(3):193–7.
- [54] Wang Q, Xue Q, Liu H, Shen W, Xu J. Wear 1996;198(1–2):216–9.
- [55] Chen CH, Jian JY, Yen FS. Composites Part A – Applied Science and Manufacturing 2009;40(4):463–8.